scientific reports

Check for updates

OPEN

A novel amphibian herpesvirus (candidate *Batravirus ranidallo5*) associated with disease in free-ranging Iberian painted frogs (*Discoglossus galganoi*) in Spain

Jaime Bosch[1], Barbora Thumsová[2], Justina Pérez-Martín[2], Carlos Caballero-Díaz[2], Roser Velarde[3], Albert Martínez-Silvestre[4], Jasmine Portmann[5,6] & Francesco C. Origgi[6,7,8]✉

Amphibians are undergoing a dramatic global decline. This massive biodiversity loss, which is critically impacting public and planetary health, has been attributed to multiple causes including infectious diseases. Of the known pathogens associated with obvious diseases in amphibians, herpesviruses have recently raised attention secondary to the discovery of two new species, both associated with skin diseases. Here, we provide the detection and characterization of a novel amphibian herpesvirus associated with a proliferative skin disease, closely resembling that previously described in association with *Batravirus ranidallo3* (previously Ranid herpesvirus 3-RaHV3) and Bufonid herpesvirus 1 (BfHV1). The novel virus, tentatively named candidate *Batravirus ranidallo5* is genetically related, but distinct from the previously described Batraviruses and it is the first amphibian herpesvirus described in Spain. The full-length genome obtained for this novel herpesvirus is approximately 220 kb and it contains the homologues of herpesvirus hallmark genes, which allows us to propose its unambiguous classification as a herpesvirus. Interestingly, a number of predicted ORFs showed to match closer to fish Alloherpesviruses homologues than Batraviruses. The discovery within a limited time span of three distinct herpesviruses, all associated with obvious skin diseases in Europe is alarming and may have significant implication for amphibian conservation.

Keywords Putative *Batravirus ranidallo5*, Frog, Amphibian, Disease, Wildlife

Infectious diseases are universally recognized stressors shown to be significant contributor of the amphibian global decline[1,2]. The dramatic loss of biomass, secondary to this decline, is translating into a major impact not only for amphibian conservation worldwide, but also for human and planetary health as it has been recently documented[3]. Additionally, to Ranavirus and Chytrids, which have been shown to be responsible of local species extirpation and extinction[4–6], novel infectious agents, namely Ranid herpesvirus 3 (now *Batravirus ranidallo3*-RaHV3) and Bufonid herpesvirus 1 (BfHV1) have been discovered and characterized during the last few years[7,8]. Although, their actual impact on the affected amphibian populations (common frogs-*Rana temporaria* and common toad-*Bufo bufo*, respectively) is not clear, evidence of a significant and potentially recurrent disease has been documented in both species[9] along with associated mortality[8]. Interestingly, we have now evidence that the associated diseases are not only confined to Switzerland, but to several European countries, potentially impacting a massive number of amphibians across Europe (Origgi, unpublished data)[10–12]. More alarming, evidence of infection at the tadpole stages, possibly impacting their survival, has been recently observed[13]. These novel amphibian herpesviruses (HVs) are invariably associated with a proliferative skin disease, which

[1]CSIC-University of Oviedo-Principality of Asturias, 33600 Mieres, Spain. [2]Asociación Herpetológica Española (AHE), 28006 Madrid, Spain. [3]Universitat Autònoma de Barcelona, 08193 Bellaterra, Spain. [4]Catalonian Reptiles and Amphibians Rescue Center (CRARC), 08783, Masquefa Barcelona, Spain. [5]Institute of Virology and Immunology, CH-3001Länggass-Str. 122, Bern, Switzerland. [6]Vetsuisse Faculty, University of Bern, microbics GmbH, Gewerbestrasse 23, CH-3012 Bern, Switzerland. [7]Institute of Microbiology, University of Applied Sciences and Arts of Southern Switzerland (SUPSI), Mendrisio, Switzerland. [8]University of Messina, Viale Giovanni Palatucci sn, 98168 Messina, Italy. ✉email: francesco.origgi@supsi.ch

is characterized by grey and brown patches respectively in frogs and toads[7–9], although, more recently PCR detection of these viruses was reported in specific lesion-free animals[12].

Interestingly, a similar, but not completely overlapping pathology phenotype has been observed in two different localities of central Spain in free ranging frogs (Iberian painted frog-*Discoglossus galganoi*) during the period 2019–2022. Our investigation shows how these lesions are associated with a novel amphibian herpesvirus, here and through the text referred as Ranid herpesvirus 5 (RaHV5). This work expands our knowledge and understanding of herpesviruses in amphibians, providing critical elements for amphibian conservations, which are fundamental not only for the preservation of biodiversity, but also for human and planetary health.

Results

Animals

In April 2019, several Iberian painted frogs (*Discoglossus galganoi*) were observed with obvious skin changes in the Guadarrama river near Villaviciosa de Odón, Madrid, Spain. Two of the observed frogs were collected alive (cases 1 and 2) and brought to the National Museum of Natural Sciences-CSIC, Madrid, for further investigation. A toe-clip from each animal was collected for molecular analyses and following they were sent alive to the Catalonian Reptiles and Amphibians Rescue Center (CRARC) for clinical and pathological evaluation. Later, in February 2021 one additional individual, was found dead with no skin abnormalities, and it was fixed in 70% ethanol in the field (case 3). In April 2022, a single individual with no visible skin changes was found dead in the same location. A toe-clip sample was collected (case 4) from this individual as well. Finally, in April 2022, one individual of the same species with similar skin changes was collected alive near Colmenar Viejo, Madrid, Spain, a locality 50 km away from the first location where frogs with tissue changes were observed initially (case 5).

Pathology

Macroscopic pathology

At postmortem examination, case 1, 2 and case 5 had approximately 20% and 50% of the body surface affected by skin lesions, respectively. Lesions consisted of multifocal-to-coalescing, grey-to-blue, shiny, well-demarcated areas of raised, thickened skin with a smooth surface (Fig. 1).

Case 4 was in an advanced stage of decomposition and had no apparent detectable skin changes.

Microscopic pathology

Histological examination could be carried out on sections available from cases 1, 4, and 5. Multifocal to coalescent areas of epidermal hyperplasia were observed in the skin, with lesions ranging from flat or plaque-like to dome-shaped-raised areas (Figs. 2 and 3). The skin was up to eight to ten times thicker than normal. The hyperplastic epithelial cells showed a looser organization and were variably enlarged and swelling with evidence

Fig. 1. Macroscopic lesions of herpesvirus-associated skin disease in live Iberian painted frogs (*Discoglossus galganoi*). Image shows multifocal to coalescent grey-blue skin patches extending over most of dorsal body surface and legs, Madrid, Spain. Left panel case 1, right panel case 5.

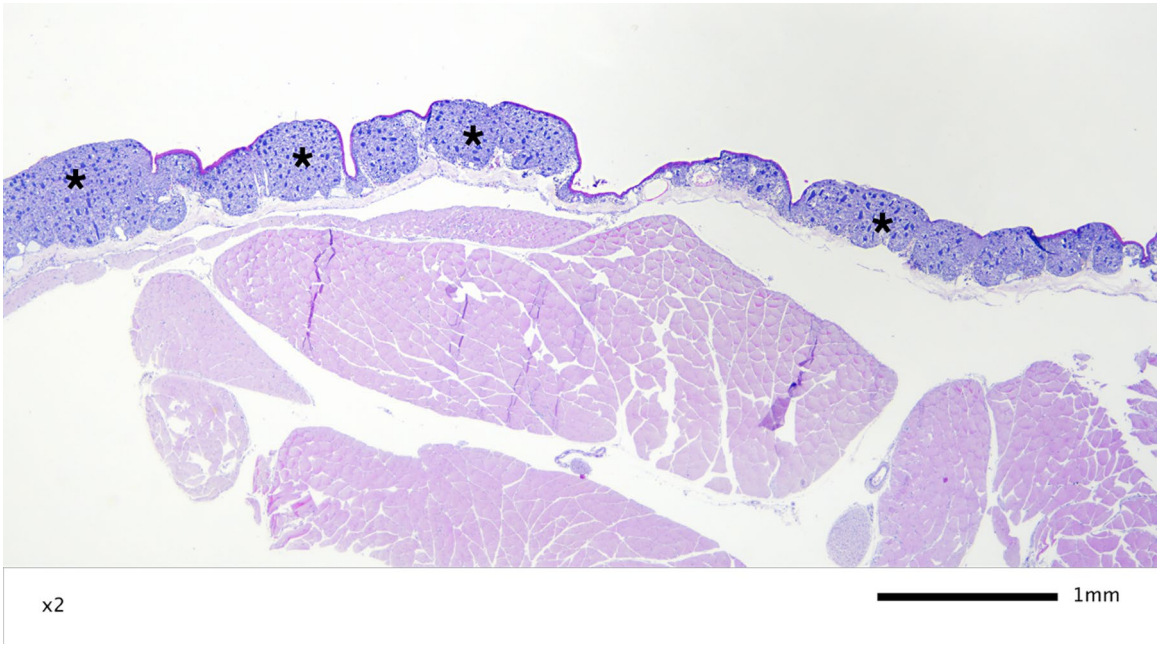

Fig. 2. Ranid herpesvirus 5 infected Iberian painted frogs (*Discoglossus galganoi*) associated microscopic skin lesions in case 5. The raised skin lesions correspond to dome-shaped-raised areas of epidermal hyperplasia (asterisks; the scale bar is shown at the bottom right of the image whereas magnification is shown at the bottom left).

of degeneration characterized by pale homogeneous to slightly granular cytoplasm (Fig. 4). Together with those interpreted as the real inclusions, characterized by large intranuclear, glassy, densely eosinophilic droplets surrounded by a clear halo (Fig. 4), occasionally present as multiple bodies per single nucleus, the infected cells showed additional peculiar morphologic elements. These appeared as variably densely packed or more loosely arranged collections of minute basophilic particles expanding in large vacuoles forming within the intercellular spaces (Figs. 3 and 4). In some degenerating keratinocytes, the cellular changes were suggestive of a progressive loss, and compression, to an extent, of cellular cytoplasm proportional to the increase of the size of the granular aggregates. In case 4, the intranuclear inclusions were particularly abundant (Fig. 4).

The cells more commonly showing cytopathic effects were disproportionally compartmentalized within the upper portion of the thickened epidermis, whereas only occasionally present in the *stratum basale*. In some instances, mucous glands were similarly affected (Fig. 2). Numerous clear sporangia consistent with Bd colonization were identified in the stratum corneum (Case 1 and 4). In the superficial dermis, only sporadic mild clusters of mononuclear inflammatory cells were noted (two spots in all sections). Lesions consistent with active Ranavirus (Rv) infections were not observed in case 5.

Ultrastructural pathology

At low magnification (Fig. 5), the large basophilic intercellular granular aggregates consisted in large collection of extracellular virions forming dense clusters surrounded by peripherally compressed epithelial cells with intact cellular membrane. These ultrastructural changes were very similar to those observed in frogs infected with *Batravirus ranidallo3*[7]. At higher magnification, many electron dense small particles were clustering within the nuclei of the infected cells where an ovoidal area of denser and darker chromatin was resembling the profile of the intranuclear inclusions observed in the hematoxylin and eosin stained sections (Fig. 6). At higher magnification (Fig. 7) large numbers of viral particles composed either of nucleocapsid alone or with a tegument, were shuttled in the cytoplasm surrounded by large vesicles (Fig. 7A). Large number of viral particles comprising an envelope as well were observed collecting into the intercellular spaces (Fig. 7B).

The morphology and the size of the particles were consistent with herpesvirus virions (Fig. 7B).

Molecular studies

Quantitative and qualitative PCR

Cases 1 2, 4 and 5 were PCR positive for Ranid herpesvirus 5 (PCR positive reaction confirmed by sequencing), whereas case 3 was not. Cases 1–2 (found alive with grey-blue patches) and case 4 (found dead with no grey-blue patches) were also PCR positive for Bd (11, 46 and 536 GC, respectively), but negative for Bsal and Rv. Case 5 (found alive with grey-blue patches) was PCR negative for Bd and Bsal, but positive for Rv (14 GC). Case 3 (found dead with no grey patches) was PCR negative for Bd, Bsal and Rv as well.

Qualitative PCR specific for known[7,8] and unknown putative Batraviruses[14] did not yield any positive result.

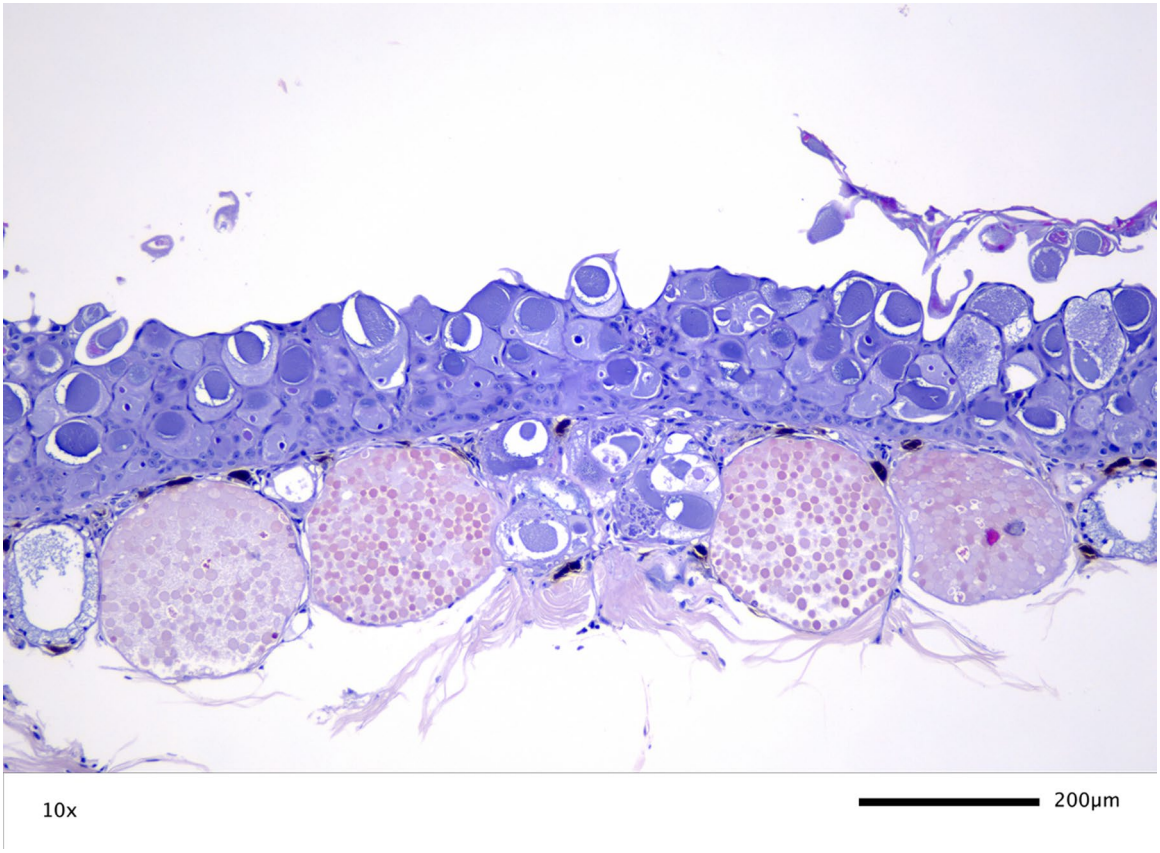

Fig. 3. Microscopic skin lesions associated with Ranid herpesvirus 5 infection in Iberian painted frogs (*Discoglossus galganoi*). The raised skin lesion corresponds to a raised flat or plaque area of epidermal hyperplasia with swollen cells and large vacuoles filled with granular basophilic material. Note the involvement of glandular structures. Case 1 (the scale bar is shown at the bottom right of the image whereas magnification is shown at the bottom left).

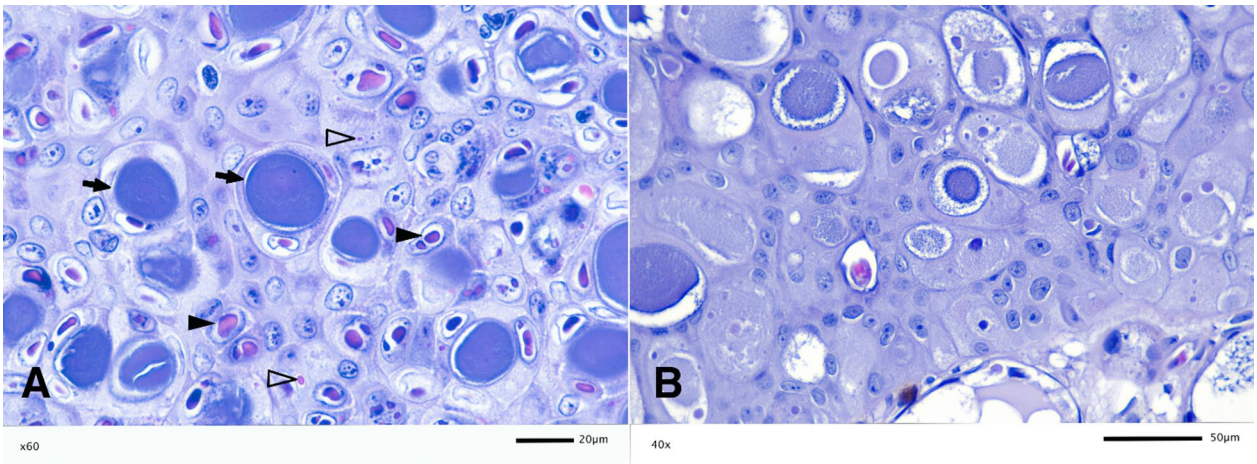

Fig. 4. Microscopic skin lesions associated with Ranid herpesvirus 5 infection in Iberian painted frogs (*Discoglossus galganoi*). (**A**) Cytopathic effects include cell enlargement and eosinophilic intranuclear inclusion bodies (solid arrowheads) and occasionally cytoplasmic eosinophilic droplets (empty arrowheads). Prominent basophilic granular aggregates (arrows) collect within the intercellular spaces. (**B**) Numerous degenerating enlarged keratinocytes with and expanding large vacuoles filled with basophilic material (A. case 5 and B. case 1; the scale bar is shown at the bottom right of the image whereas magnification is shown at the bottom left).

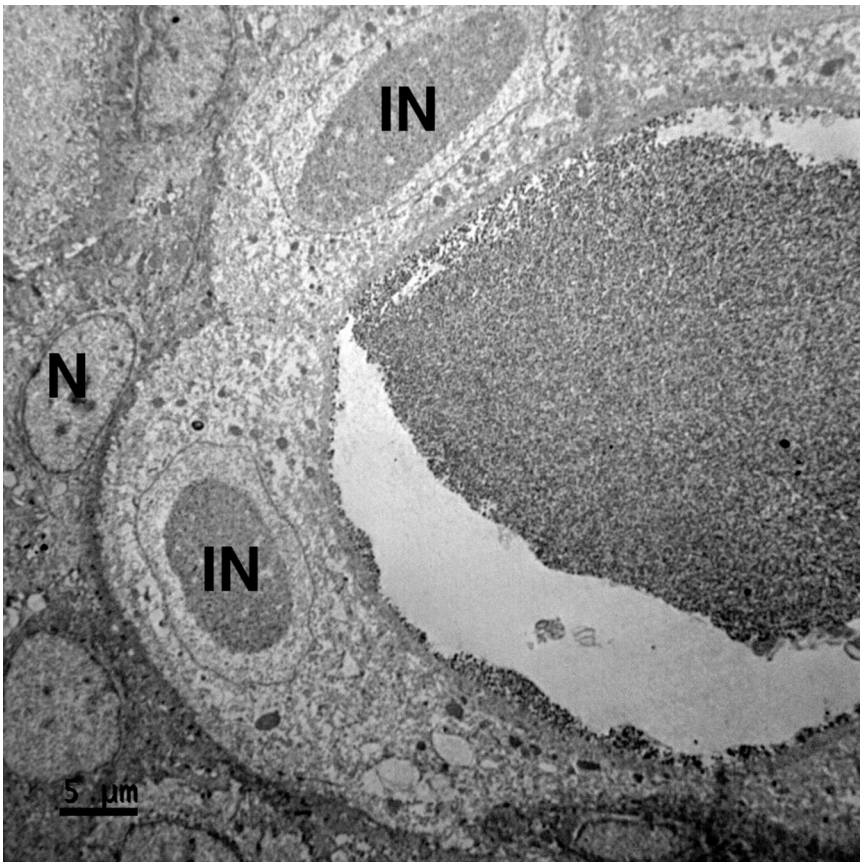

Fig. 5. Electron micrograph showing two keratinocytes infected with Ranid herpesvirus 5. The image displays putative intranuclear inclusions and an accumulation of virions in the extracellular space between cells, corresponding to the vacuoles filled with basophilic granular material shown in Figs. 3 and 4. The nucleus of an infected cell (IN) is larger than the nuclei of adjacent uninfected cells (N) and exhibits a granular karyoplasm, with increased density in the center (putative viral inclusion).

Next (NGS) and third (TGS) generation sequencing results with genome assembly

Illumina sequencing yielded a total of 4,943 Mb reads. A total of 16,475,544 clusters fulfilled the default Illumina quality criteria. A total of 89.80% of bases (PF) had a quality score greater or equal to 30. The mean quality of the nucleotide passing filter was 35.16. TGS (Nanopore Oxford technology) provided 59 batches for a total of 4,000 reads each ranging from 200 to 24,000 nt. The final construct accounted for a total of 221,649 nucleotides (nt-GenBank accession number PV243667). All the ORFs longer than 270 nt were mapped and considered further. The genome is flanked by two almost identical direct repeats measuring 84 (5') and 60 n (3'), respectively. A total of 203 ORFs were detected in the assembled genome Ranid herpesvirus 5 (GenBank Accession number PV243667). Of these, thirty-eight showed similarities with homologous amino acid (AA) sequences of other Alloherpesviruses and, for two of the predicted genes, with mammalian herpesviruses (see Supplementary Table 1). Open reading frames ranged from 270 nt up to 7,065 nt (ORF63). Among the identified putative ORFs we identified homologous of several of the genes encoding for the most conserved protein among herpesviruses, including the DNA polymerase (ORF82, 48% homologous to *Batravirus ranidallo1* (RaHV1) ORF73), terminase (72% homology to RaHV1 ORF20), the helicase (ORF52, 54% homologous to the RaHV3 ORF62) and the Major Capsid Protein (ORF34, 46% homologous to RaHV1 ORF54). Eight putative ORFs, whose homology to other herpesviruses could not be found (ORFs 8, 42, 61, 70, 106, 121, 128), were found to encode for presumptive immunomodulatory molecules including anti-apoptotic factors, MHC and T-cell receptor-like elements and TNF receptor-associated molecules. All these data are summarized in Supplementary Table 1.

Phylogenetic analysis

The phylogenetic analysis unambiguously clustered all the known Batraviruses to date with the single exception of the novel RaHV5. Interestingly, this new herpesvirus showed a more ambiguous positioning in comparison with the other Batraviruses, exactly between the Batraviruses and fish Alloherpesviruses (Fig. 8). This is consistently shown using both, the DNA polymerase (data not shown) or the Major Capsid Protein amino acid sequences. Furthermore, these data are consistent with the observed relatively high homology between several of the putatively identified encoded protein by RaHV5 and the Alloherpesviruses homologous.

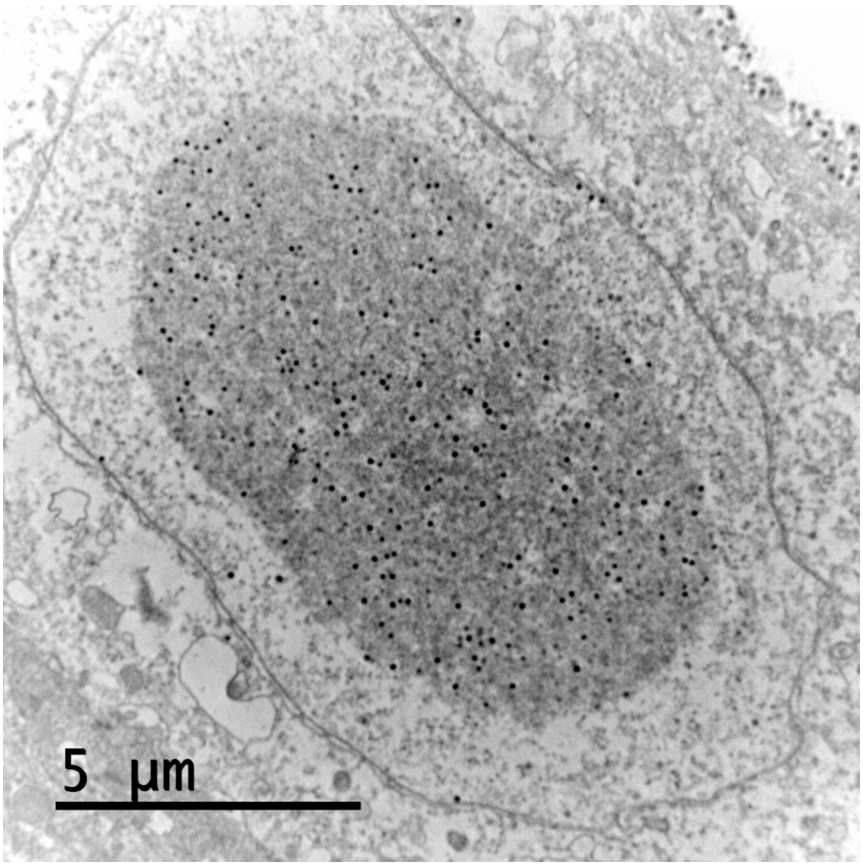

Fig. 6. Electron micrograph showing the nucleus of an infected keratinocyte with Ranid herpesvirus 5. The putative intranuclear inclusion consist of a dense electrondense material embedding numerous nucleocapsids).

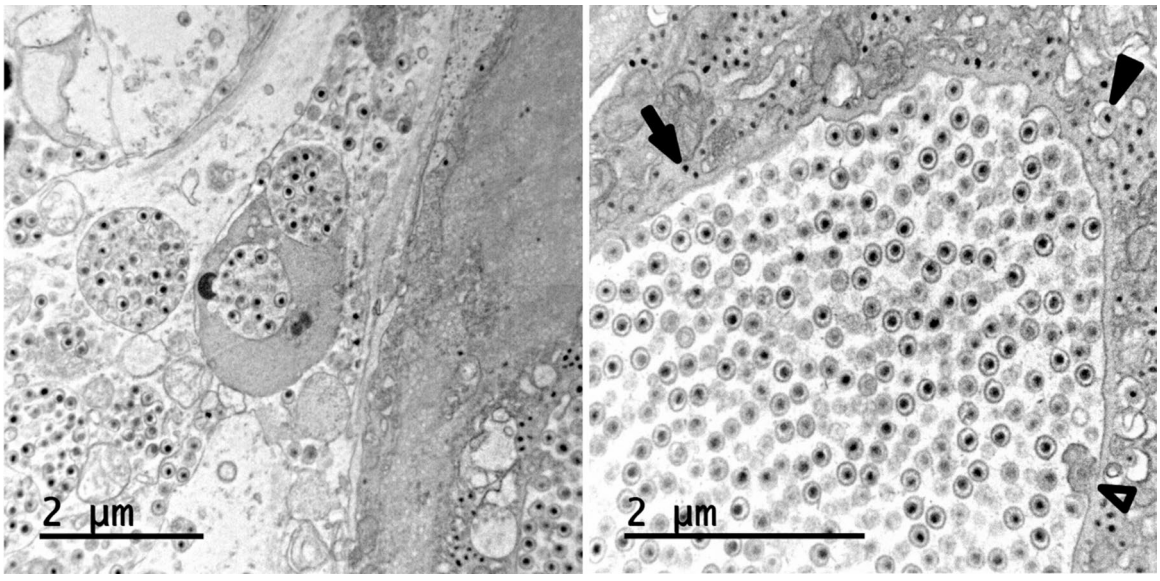

Fig. 7. Electron micrograph of the cytoplasm of a keratinocyte infected with Ranid herpesvirus 5. Virions are mostly collected into cytoplasmic membranes (left panel). Different stages of maturation of the viral particles are shown in this image (right panel), ranging from naked capsids (arrow) to capsids surrounded by presumptive tegument (solid arrowhead) and budding virions acquiring the envelope (empty arrowhead). Large number of mature viral particles are present in the extra-cellular spaces (right panel).

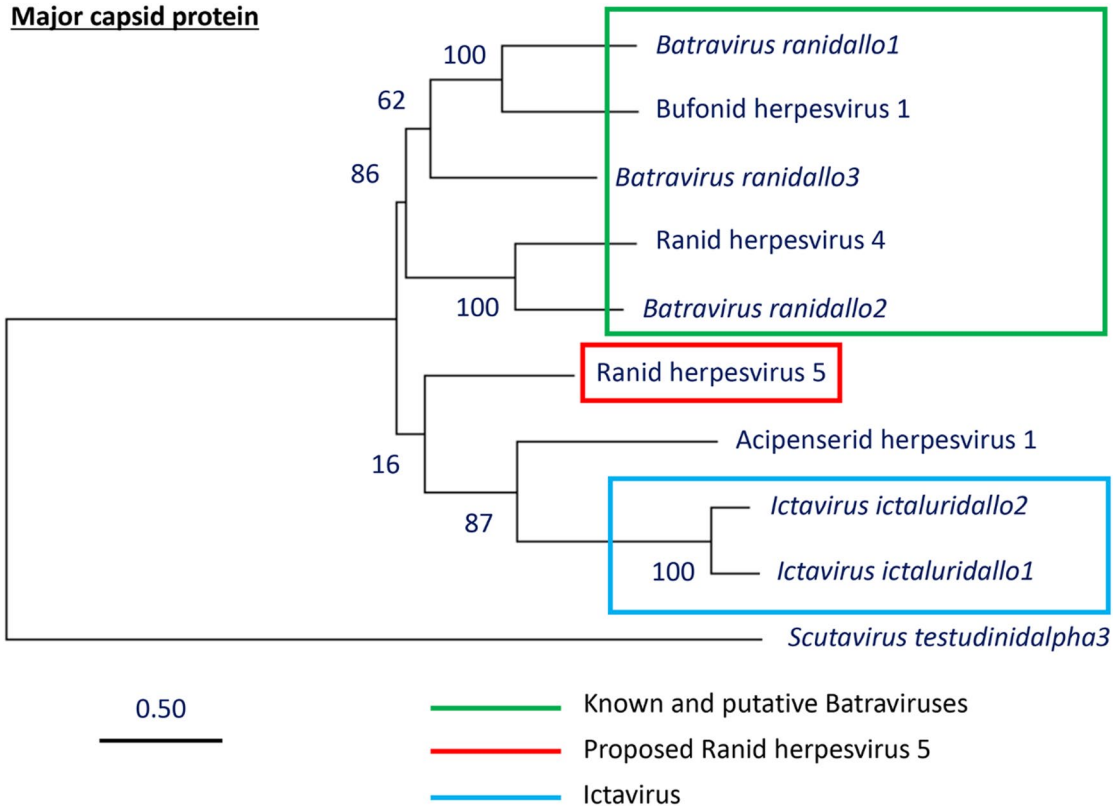

Fig. 8. Phylogenetic analysis. The maximum likelihood tree built with the amino acid sequences of the Major Capsid Protein shows a clear clustering of all the Ranid herpesviruses characterized to date (including the not clinically characterized Ranid herpesvirus 4) consistent with the current classification of the Batraviruses. Ranid herpesvirus 5 clusters separately both from the known Batraviruses and the other Alloherpesviruses. Bootstrap values are shown at the tree nodes. The length of each branch is proportional to the genetic changes, which have occurred over time. The scale bar corresponds to 50% genetic difference. The recognized species by the ICTV are written in italics.

Discussion

This investigation describes an obvious skin pathology associated with the intralesional presence of a previously undescribed herpesviruses in free ranging frogs in Spain. This is the third novel herpesvirus discovered in free ranging amphibians within the last decade and within a temporal interval of seven years[7–9], besides an additional one documented in China by metagenomics with unknown clinical significance[15]. The skin changes associated with the presence of Ranid herpesvirus 5 (candidate *Batravirus ranidallo5* according to the newly introduced nomenclature for herpesvirales) are similar to those previously described in association with *Batravirus ranidallo3* and Bufonid herpesvirus 1 in frogs and toads, respectively. Macroscopically, the distinct light blue pigmentation of the hyperplastic skin patches in the affected frogs in Spain differed from the grey and brown patches observed with RaHV3 and BfHV1 infected animals, respectively. Under light microscopy, the massive hypertrophy of the affected epithelial cells in RaHV5 affected frogs, was not obvious in RaHV3 and BfHV1 infected amphibians. The affected cells are characterized by a massive collection of dark basophilic granular material within the intercellular spaces, which increasing in size, leads progressively to the peripheral compression of the epithelial cells themselves with progressive degeneration of the infected cells. These massive granular collections consisted in myriads of virions budding out from the infected cells into the extracellular spaces. This is a feature that was observed as well in the epidermis of frogs infected with RaHV3, although to a far smaller extent, whereas no similar changes were observed in common toads infected with BfHV1. Interestingly, RaHV5 viral particles appears to be shuttled by variably sized vesicles within the cytoplasm of infected cells similarly to RaHV3, but not BfHV1-infected cells[9]. Consistently with frogs and toads infected with RaHV3 and BfHV1, respectively, the virtual absence of an obvious cellular immune response in the affected areas was observed in RaHV5-infected frogs as well.

RaHV5 is a herpesvirus with a genome of approximately 220 kb, a size that is within the typical range of Batraviruses and Alloherpesviruses (Genbank Accession number PV243667). Our investigation led to the identification of homologues of herpesvirus hallmark genes in the genome of RaHV5, which allows us to propose its unambiguous classification as a herpesvirus. Interestingly, large numbers of predicted ORFs could not be associated with homologous ones from other Batraviruses and even more interesting, a number of predicted ORFs showed to match closer to fish Alloherpesviruses homologues than Batraviruses.

Despite this possible intriguing phylogenetic positioning, it is clear that a striking overlapping pathogenesis is shared by all the European amphibian herpesviruses characterized to date. They are all associated with localized proliferative skin diseases in absence of any obvious cellular immune response, independently of the host. These features differentiate them from the two American amphibian herpesviruses (RaHV1 and-2), which are characterized by a distinct pathogenesis, with RaHV1 causing a renal adenocarcinoma in the affected frogs and RaHV2 instead causing possible disease only in larvae (edema)[16,17].

Interestingly, the affected frogs from Spain were coinfected with other agents (either Bd or Rv) and it is not clear at all the contribution, if any, of herpesvirus to the susceptibility to other agents (or the other way around) and to their impact on the affected host.

Interestingly, the *Discoglossus* genus, along with the entire Alytidae family, to which it belongs, is highly susceptible to both chytridiomycosis and ranavirosis[18–21]. Therefore, the emergence of a new pathogen in Iberia affecting this highly susceptible group of amphibians, where five out of the seven existing species are endemic, is of great concern. Furthermore, the PCR positivity of individuals not showing clinical signs suggests that the virus might be far more diffused than our preliminary data might suggest.

Along this line, the discovery of three novel amphibian herpesviruses in seven years is alarming. Since our first reporting of the novel RaHV3 and BfHV1 an increase interest has risen on amphibian herpesvirus and likely more attention has been paid to skin abnormalities observed in frogs and toads. However, this is most likely only one part of the explanation. Accordingly, we cannot rule out that additional factors might have contributed to the surfacing of these diseases and associated viruses.

It is now obvious, that herpesviruses are important and globally diffused infectious agents of amphibians. It is very likely that several others will be discovered and characterized in the near future. However, while proceeding with the characterization and description of these agents and their associated diseases, it is imperative to question the actual significance of these observations for amphibian survival, conservation and planetary health. It is of major concern to think of these agents and their associated diseases, not only as a threat for the affected species but as well, as a sign of a progressive global environmental imbalance calling the whole scientific community to respond and act accordingly.

Materials and methods

Animals

All experimental protocols were approved by the CSIC ethics committee (https://www.csic.es/en/csic/research-integrity-and-ethics-csic/csic-ethics-committee). All the "hands-on" animal procedure were carried out under the permit n. MBCFS-06–23 issued by the Government of Catalonia. Finally, all the methods applied were in accordance with the ARRIVE guidelines (https://arriveguidelines.org).

Pathology

All frogs submitted alive (case 1, 2 and 5) were humanely euthanized with an overdose MS222 (Tricaine Pharmaq 1000 mg/g; Zoetis Spain, Madrid, Spain) according to established guidelines (https://www.aaalac.org/accreditation/RefResources/SS_Amphib.pdf). Animals were fixed in buffered formalin (4%) for 48 h and decalcified using a fixative containing formic acid (*Casa Alvarez*, ref. 10–6113, Barcelona, Spain). Tissues from these individuals underwent processing and paraffin embedding, to be then sectioned 4 µm thick and stained with hematoxylin and eosin (H&E) according to standard protocols. Skin tissue samples obtained from case 1, originally formalin fixed, were then fixed in 2.5% glutaraldehyde and processed for transmission electron microscopy (TEM) (please, see below).

Electron microscopy

Skin tissues were first fixed with 2.5% glutaraldehyde in cacodylate 0.1 M ON at 4 °C and then post-fixed with 1% osmium tetroxide with 0.8% potassium ferrocyanide for 2 h and finally dehydrated in increasing concentrations of acetone. Following, tissues were embedded in epon resin (EMS, Hatfield, PA, USA) and polymerized at 60 °C for 48 h. Seventy nm thick sections were obtained with a Leica EM UC6 ultramicrotome. Sections were double stained with 1% uranyl acetate for 45 min (Sigma Aldrich, Steinheim, Germany) and 3% lead citrate for 5 min at 20˚C in an automatic contrasting system Leica EM AC20. Sections were then examined under a JEM-1400 transmission electron microscope (JEOL, Akishima, Tokyo, Japan), and images were taken at a voltage of 120 kV.

Molecular studies

DNA extractions

DNA was obtained from toe clips or whole tissues (not yet fixed in formalin) obtained from the frog carcasses (Qiagen DNeasy kit, Hilden and Germany) according to the specific manufacturer's instructions. DNA was quantified using a Qubit fluorometer (Thermo Fischer Scientific, Zurich, CH) according to the manufacturer's instructions.

Next generation sequencing (NGS-Illumina platform)

Total DNA obtained from cases 1–5 were pooled and three micrograms of total DNA was delivered to a biotech (Fasteris SA, Geneva, CH) for deep sequencing to be carried out on an Illumina platform (Illumina NovaSeq 6000). The template was sequenced at a depth of 100mio reads following an established protocol[7,8,22].

Third generation sequencing (TGS-MiniION platform)

The same amount of total DNA underwent deep sequencing using an in house MiniION platform. Following library preparation (SQK-LSK109 1D ligation genomic DNA, Oxford Nanopore Technology, Oxford, UK), to create a sequencing library the purified gDNA was first nickase/end-repair treated. The reaction consisted of 3.5

µL Ultra II End-prep reaction buffer (NEB E7546), 3.5 µL FFPE DNA repair buffer (NEB M6630S), 3 µL Ultra II End-prep enzyme mix (NEB), 2 µL FFPE DNA repair mix (NEB), 1 µL DNA Control (CS, ONT), 17 µL gDNA (212,5 ng) and nuclease-free water to make a total volume of 60 µL. The mixture was incubated at 20 °C for 5 min and 65 °C for 5 min. An AMPure XP bead clean-up was performed (Beckman Coulter) before sequencing adaptors were ligated to the double-stranded DNA. Ligation was then performed by adding 5 µL Adaptor Mix (AMX, ONT), 25 uL Ligation Buffer (LNB, ONT) and 10 µL NEBNext Quick T4 DNA Ligase (NEB E6056) to the 60 µL dA-tailed DNA. The reaction was incubated for 10 min at room temperature before further purification using AMPure XP beads. Short Fragment Buffer (SFB, ONT) was used to wash the beads prior to elution in 15 µL Elution Buffer (EB, ONT), gently mixed and incubated at room temperature for 10 min. Fifty fmol of library (12 µL) was added to 37.5 µL Sequencing Buffer (SQB, ONT) and 15.5 µL Loading Beads (LB, ONT) and loaded into a primed R9.4.1 flow cell. A 36 h sequencing run was initiated using MinKNOW v.1 software (ONT).

Genome assembly

The reads batches, obtained with Nanopore technology were *de novo* assembled using the software Geneious prime version 2023.2.1 (Dotmatics, Boston, MA, USA). A total of 506 assemblies were obtained ranging from 2,745 to 66,893nt, which were all manually assessed. All the assemblies were blasted (BLASTX, NCBI) and four redundant sequences showing homologies with amphibian herpesviruses were obtained. These four sequences were used as templates to map the reads obtained with the Illumina platform. Mapping was carried out using Geneious prime 2023.2.1 with 25 to 100 iterations. Four large contigs ranging from 39,316 to 68,871 nt were obtained. The obtained contigs showed obvious gaps between each other. In order to fill the gaps, all the reads obtained by TGS were mapped towards the four obtained large contigs, one at a time, using the Geneious software, with 1 to 5 iterations. At the end of each iteration run we manually checked, for each contig, if overlapping sequences with any of the other three remaining contigs were obtained. Once an overlap was detected, the two corresponding contigs were then joined. The combined contig was then newly mapped against the Illumina reads to correct all the TGS ambiguous nucleotides. We repeated the procedure until all the four contigs could be integrated in a single one spanning across the entire genome of the newly detected virus. Finally, considering that herpesviruses undergo circling early in their replication (rolling cycles), we checked for overlapping sequences at the extremities of the single contigs, which we finally found.

Real time PCRs

Presence of *Batrachochytrium dendrobatidis* (Bd) and *B. salamandrivorans* (Bsal) DNA was investigated by real-time Taqman PCR (MyGo Pro machine) according to the protocols by Blooi et al.[23] (Bd primers: ITS1-3: 5'-C CTTGATATAATACAGTGTGCCATATGTC-3', 5.8 S: 5'-AGCCAAGAGATCCGTTGTCAAA-3'; FAM-labeled TaqMan probe for Bd: 5'-CGAGTCGAACAAAAT-3'; Bsal- primers: STerF: 5'-TGCTCCATCTCCCCCTCTT CA-3', STerR: 5'-TGAACGCACATTGCACTCTAC-3'; NED-labeled TaqMan probe for Bsal: 5'-ACA AGAAA ATACTATTGATTCTCAAACAGGCA-3') and for detection of *Ranavirus* (Rv) according to the protocol by Leung et al.[24] DNA (Rv primers- MCP_F: 5'-GTCCTTTAACACGGCATACCT-3', MCP_R: 5'-ATCGCTGGTG TTGCCTATC-3'; VIC-labeled TaqMan probe for Rv: 5'-TTATAGTAGCCTRTGCGCTTGGCC-3'). All samples were run in duplicate together with negative and positive controls with known concentrations of target genes copy numbers (GC; from 1 to 10,000,000 in log10 increments). The cycle threshold (CT) used as cutoff was 37 for all the three targets (Bd, Bsal, Rv). A sample was considered positive when both replicates showed a robust sigmoidal amplification signal, and the infection load was equal to or higher than the lower positive control. If just one of the two replicates was amplified successfully, the specific sample was analyzed a third time and considered positive only if the curve of the third amplification could be deemed as positive according to the parameters listed above.

Qualitative PCRs

Total DNA from the affected frogs underwent qualitative PCR amplification as well using an established protocol previously developed, including specific PCR settings for Ranid herpesvirus 3 (*Batravirus ranidallo3*),[7] for Bufonid herpesvirus 1[8] and consensus PCR protocols developed to amplify all the known Batrachoviruses to date[14]. Finally, a RaHV5 specific qualitative PCR protocol was developed targeting the partial sequence of the DNA polymerase gene (amplicon = 262nt long). Forty pmol each of forward (5'- AAG CTA GAC AAA AGC GAC TGC C-3') and reverse (5'- ACC TG G T TT ACT TG T A AT TGT CC-3') primers were added to a reaction mix composed of 3 µl of 10x reaction buffer, 3.75 µl of $MgCl_2$ (25 Mm), 0.4 µl of a 10mM dNTPs mix, 0.2 µl (1U) of FIREpol DNA polymerase (Solis biodyne, Lucerna Chem, Luzern, Switzerland), and distilled deionized water with a final volume of 30 µl. The cycling reaction was carried out on an Applied Biosystems Thermocycler 9600 Fast (Applied Biosystems, Foster City, Canada). The cycling protocol consisted of an initial denaturation step at 95 °C for 3 min followed by 35 cycles including a denaturation step at 95 °C for 30 s, an annealing step at 50 °C for 30 s, and an elongation step at 72 °C for 60 s. A final elongation at 72 C for 10 min was then carried out . The obtained amplicon was then resolved in a 1.5% agarose gel and examined under ultraviolet light.

Phylogeny

The amino acid sequences of the putative homologous of the Major Capsid Protein were used to construct a maximum likelihood phylogenetic tree together with the homologous sequences from Ranid herpesvirus 1, 2, 3 (*Batravirus ranidallo1*, *2*, *3*-GenBank Ref. Numbers YP656709.1, YP656588.1, YP009362419.1) and 4 (GenBank Ref. Number QWY26478.1), Bufonid herpesvirus 1(GenBank Ref. Number YP009552946.1), Acipenserid herpesvirus 1 (GenBank Ref. Number UKB92887.1), Ictalurid herpesvirus 1 and 2 (now *Ictavirus ictaluridallo1* and *2*-GenBank Ref. Numbers NP041130.1, YP009447864.1) and *Scutavirus testudinalpha3* as outgroup

(GenBank Ref. Number AKV40691.1). The sequences were fed to the program Mega 7 (Molecular Evolutionary Genetics Analysis version 7.0 for bigger datasets)[25], using standard settings and performing 10,000 replicates.

Data availability

All the data concerning this investigation are reported in this article, in the associated supplemental material and in the Genbank database (accession number [PV243667](https:/www.ncbi.nlm.nih.gov/genome/?term=PV243667)).

Received: 16 July 2025; Accepted: 17 October 2025
Published online: 21 November 2025

References

1. Catenazzi, A. State of the world's amphibians. *Ann. Rev. Envir Res.* **40**, 91–119 (2015).
2. Skerratt, L. F. et al. Spread of chytridiomycosis has caused the rapid global decline and extinction of frogs. *EcoHealth* **4**, 125–134 (2007).
3. Springborn, M. R., Weill, J. A., Lips, K. R., Ibáñez, R. & Ghosh, A. Amphibian collapses increased malaria incidence in Central America. *Environ. Res. Lett.* **17**(10), 104012 (2022).
4. Bosch, J., Martínez-Solano, I. & García-París, M. Evidence of a Chytrid fungus infection involved in the decline of the common midwife Toad (*Alytes obstetricans*) in protected areas of central Spain. *Biol. Conserv.* **97**, 331–337 (2001).
5. Stegen, G. et al. Drivers of salamander extirpation mediated by *Batrachochytrium salamandrivorans*. *Nature* **544**, 353–356 (2017).
6. Price, S. J. et al. Collapse of amphibian communities due to an introduced *Ranavirus*. *Curr. Biol.* **24**, 2586–2591 (2014).
7. Origgi, F. C. et al. *Ranid Herpesvirus 3* and proliferative dermatitis in free-ranging wild common frogs (*Rana temporaria*).. *Vet. Pathol.* **54**, 686–694 (2017).
8. Origgi, F. C. et al. *Bufonid herpesvirus 1* (BfHV1) associated dermatitis and mortality in free ranging common toads (*Bufo bufo*) in Switzerland. *Sci. Rep.* **8**(1), 14737 (2018).
9. Origgi, F. C. et al. Herpesvirus-associated proliferative skin disease in frogs and toads: proposed pathogenesis. *Vet. Pathol.* **58**, 713–729 (2021).
10. Eisenberg et al. Emergence of a Bufonid herpesvirus in a population of the common Toad Bufo Bufo in Germany. *Dis. Aquat. Org.* **145**, 15–20 (2021).
11. Franklinos, L. H. V. et al. Herpesvirus skin disease in free-living common frogs Rana temporaria in great Britain. *Dis. Aquat. Org.* **129**, 239–244 (2018).
12. Leineweber, C. et al. Detection of bufonid herpesvirus 1 and Ranid herpesvirus 3 in native amphibians in Schleswig-Holstein, Germany, 2022–23. *J. Wild Dis.* **6**, 767–772 (2025).
13. Origgi, F. C. & Taugbøl, A. Ranid herpesvirus 3 infection in common frog *Rana temporaria* tadpoles. *Emerg. Infect. Dis.* **29**, 1228–1231 (2023).
14. Licheri, M. & Origgi, F. C. Consensus PCR protocols for the detection of amphibian herpesviruses (*Batrachovirus*). *J. Vet. Diagn. Invest.* **32**, 864–872 (2020).
15. Chen, X. X., Wu, W. C. & Shi, M. Discovery and characterization of actively replicating dna and retro-transcribing viruses in lower vertebrate hosts based on rna sequencing. *Viruses* **13**(6), 1042 (2021).
16. McKinnell, R. G. The Lucké frog kidney tumor and its herpesvirus. *Am. Zool.* **13**, 97–114 (1973).
17. Rafferty, K. A. in *Jr. Renal Neoplasia*. 311–315 (eds King, J. S.) (Brown, 1967).
18. Bosch, J. et al. Long-term monitoring of amphibian populations of a National Park in Northern Spain reveals negative persisting effects of Ranavirus, but not *Batrachochytrium dendrobatidis*. *Front. Vet. Sci.* **8**, 645491 (2021).
19. Martínez-Silvestre, A. et al. Introduced mediterranean painted frogs (*Discoglossus pictus*) are possible supershedders of the fungus *Batrachochytrium dendrobatidis* in Catalonia (NE Spain). *Amphibia-Reptilia* **51**, 1–5 (2023).
20. Thumsová, B., Donaire-Barroso, D., Mouden, E. & Bosch, E. H. Fatal chytridiomycosis in the Moroccan midwife Toad *Alytes Maurus* and potential distribution of *Batrachochytrium dendrobatidis* across Morocco. *Afr. J. Herpetol.* **71**, 72–82 (2022).
21. Thumsová, B., Bosch, J. & Rosa, G. M. in *Evolutionary Ecology of Amphibians*. 54–102 (eds Moreno-Rueda, G. & Comas, M.) (CRC, 2023).
22. Origgi, F. C. et al. A genomic approach to unravel Host-Pathogen interaction in chelonians: the example of testudinid herpesvirus 3. *PLoS ONE*. **10**, e0134897. https://doi.org/10.1371/journal.pone.0134897 (2015).
23. Blooi, M. et al. Duplex real-Time PCR for rapid simultaneous detection of *Batrachochytrium dendrobatidis* and *Batrachochytrium salamandrivorans* in amphibian samples. *J. Clin. Microbiol.* **51**, 4173–4177 (2013).
24. Leung, W. T. M. et al. A quantitative-PCR based method to estimate ranavirus viral load following normalisation by reference to an ultraconserved vertebrate target. *J. Virol. Methods*. **249**, 147–155 (2017).
25. Kumar, S., Stecher, G. & Tamura, K. MEGA7: molecular evolutionary genetics analysis version 7.0 for bigger datasets. *Mol. Biol. Evol.* **33**, 1870–1874 (2016).

Acknowledgements

We thank I. Acevedo, A. Gorge-García, and C. Sausor for laboratory assistance and A. Martín for field assistance. BT was supported by 'Doctorados Industriales de la Comunidad de Madrid' (Ref. IND2020/AMB-17438). The Consejería de Medio Ambiente of Comunidad de Madrid extended the permit for field work (ref. 10/171706.9/21). The authors would like to thank the staff from the Servei de Microscòpia i Difracció de Raigs X of Universitat Autònoma de Barcelona.

Author contributions

JB was responsible for the conception and design of the study, supervision of the research, contribution to the data collection, analysis and interpretation, to the writing and critically revision of the manuscript. BT Contributed to the data analysis and interpretation, writing and critically reviewing the manuscript. JPM and CCD contributed to the data collection and critically reviewed the manuscript. RV Performed the pathology and contributed to the TEM, to the writing and critical revision of the manuscript. AMS performed the pathology investigation, contributed to the TEM and to the writing and critical revision of the manuscript. JP Contributed to the genome sequencing (MinION) and critically reviewed the manuscript. FCO Contributed to the coordination of the investigation, experimental design, data analysis and interpretation, sequenced and assembled the viral genome, and wrote the manuscript. The final version of this manuscript was seen and approved by all the authors.

Declarations

Competing interests
The authors declare no competing interests.

Additional information
Supplementary Information The online version contains supplementary material available at https://doi.org/10.1038/s41598-025-25189-9.

Correspondence and requests for materials should be addressed to F.C.O.

Reprints and permissions information is available at www.nature.com/reprints.

Publisher's note Springer Nature remains neutral with regard to jurisdictional claims in published maps and institutional affiliations.